Algerian Journal of Chemical Engineering

Algerian Journal of Chemical Engineering
EISSN: 2773-3068 (Online)
DOI: ***10.5281/zenodo.20743173***
Fatiha. I et al / vol. 01, n°1 - 2026

Original Article **Open Access**

Nonlinear Numerical Modeling of Prestressed Concrete Beams with Variable Sectional Stiffness

Fatiha. Iguetoulene , Youcef. Bouafia and Mohand .Said. Kachi

[a] University Mouloud Mammeri of Tizi-Ouzou , Civil Engineering, 15000 Algeria ; *iguetoulene_fatiha@yahoo.fr*
[b] *University Mouloud Mammeri of Tizi-Ouzou , Civil Engineering, 15000 Algeria; Youcef.bouafia2012@yahoo.com*

[c] *University Mouloud Mammeri of Tizi-Ouzou , Civil Engineering, 15000 Algeria; kachi ms@yahoo.fr*

* *Corresponding author.* E-mail address: iguetoulene_fatiha@yahoo.fr
Article history: Received 28 February 2026, Revised 16 *June 2026, Accepted* 18 *June 2026*

ABSTRACT

This paper presents a nonlinear finite element formulation for the analysis of prestressed concrete beams under different loading conditions. Particular attention is devoted to the modeling of prestressing effects, incorporated into the sectional stiffness matrix through an incremental variable-stiffness approach. The formulation also accounts for material nonlinearity and second-order effects using two-node beam elements combined with Simpson's integration scheme. The proposed model is based on the principle of virtual work and includes constitutive modeling of concrete and prestressing steel materials. Numerical predictions were validated against experimental results obtained from prestressed concrete beams. Good agreement was observed between numerical and experimental results in terms of load-deflection response, nonlinear behavior, and overall structural performance.
The results demonstrate the accuracy and reliability of the developed formulation, showing its effectiveness as a numerical tool for the analysis and design of prestressed concrete beams.
Keywords: Prestressed concrete beams, section stiffness matrix , Virtual work principle, Constitutive modeling, displacements .

1. Introduction

The rapid development of computer tools and numerical techniques has profoundly transformed the field of civil engineering, particularly in the analysis of prestressed concrete structures. Nonlinear analysis methods applied to prestressed concrete structures have experienced considerable growth in recent years due to advances in computer technology. These methods make it possible to represent with great accuracy the actual behavior of structures up to failure, taking into account complex phenomena such as large displacements, cracking, plastic deformation, and significant stress redistributions. as discussed by [1–2,5,7]. The consideration of prestressing in the formulation of

Algerian Journal of Chemical Engineering
EISSN: 2773-3068 (Online)
DOI: 10.5281/zenodo.20743173
Fatiha. I et al / vol. 01, n°1 - 2026

the section stiffness matrix is essential in the analysis of prestressed concrete structures, due to its significant influence on the distribution of stresses and internal forces within the structure [1–13]. These studies emphasize the importance of considering both the global structural response and the local behavior each element simultaneously. Significant research efforts have been devoted to improving nonlinear analysis procedures, particularly in the formulation of the tangent stiffness matrix. Methods proposed by [10] have contributed substantially to this field. However, these approaches may fail to capture high-frequency modes accurately and can result in non-symmetric tangent stiffness matrices. In this paper, a numerical formulation based on the principle of virtual work is presented to model and analyze the nonlinear structural response under external loading [12]. The governing equilibrium equations are derived, and the solution procedure for these equations is discussed. Constitutive laws for concrete and reinforced concrete are then introduced, this study focuses on the introduction of the prestressing effect into the nonlinear analysis of structures, particularly in the formulation of the section stiffness matrix [04]. For solving the problem, a displacement-based method with variable stiffness is used. The main features of this method are presented in this paper, a numerical formulation based on the principle of virtual work is presented to model and analyze the nonlinear behavior of prestressed concrete beams and reinforced concrete truss beams under external loads. The analysis accounts for the actual behavior of concrete and steel, including cracking, steel yielding, and failure mechanisms. A nonlinear calculation program developed in Fortran.

In this study, particular attention was given to the incorporation of prestressing effects into the sectional stiffness formulation, as well as to the extension of the model to different structural idealizations within a unified numerical framework. In addition, the effects of prestressed concrete were incorporated into the sectional stiffness matrix.

2. Material and methods

2.1 Behavior of Materials

2.1.1 Concrete in Compression and Tension

The behavior of concrete in compression is described by Sargin's law, as presented in reference [01, 5,8].

the tensile behavior will be modeled by the law of Grelat [8]

.

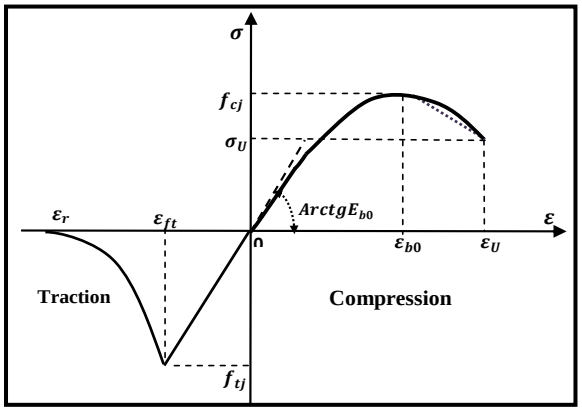

Figure 1 constitutive law of the concrete

Algerian Journal of Chemical Engineering
EISSN: 2773-3068 (Online)
DOI: 10.5281/zenodo.20743173
Fatiha. I et al / vol. 01, n°1 - 2026

$$\boldsymbol{\sigma} = f_{cj}\frac{k_b.\bar{\varepsilon}+(k_b'-1)\bar{\varepsilon}^2}{1+(k_b-2)\bar{\varepsilon}+k_b'\bar{\varepsilon}^2} \qquad (1)$$

With

$$\bar{\varepsilon} = \frac{\varepsilon}{\varepsilon_{b0}},\ k_b = \frac{E_{b0}\,.\varepsilon_{b0}}{f_{cj}}$$

2.1.2 Steel

The stress–strain behavior of steel under monotonic loading is assumed to be the same in tension and compression. The steel materials considered in this study consist of passive reinforcement and prestressing steel.

- **Passive Reinforcement Steels**

Passive reinforcement steels are classified into two types:

- natural steels
- strain-hardened (cold-worked) steels

Natural steels are characterized by an ideal elastic–plastic behavior law.

Natural Steels

For natural steels, the ideal elastic–plastic constitutive law is written as:

$$\sigma = E_s\,\varepsilon \ \text{ for } \ 0 \le \varepsilon < \frac{\sigma_e}{\gamma_s E_s}$$

$$\sigma = \frac{\sigma_e}{\gamma_s} \ \text{ for } \ \varepsilon \ge \frac{\sigma_e}{\gamma_s E_s} \qquad (2)$$

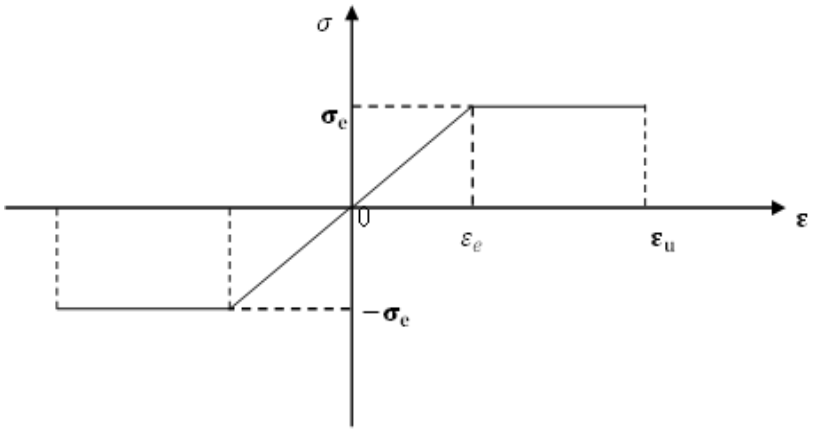

Figure 2 Stress–strain diagram of natural steel

-Strain-hardened steels

Cold-worked steels follow the BAEL model, which assumes an elastic behavior up to 70% of the yield stress, a nonlinear fifth-degree curve up to about 1% strain, and a constant stress plateau beyond this range up to approximately 4% strain, with a symmetric stress–strain diagram composed of linear and nonlinear parts.

Algerian Journal of Chemical Engineering
EISSN: 2773-3068 (Online)
DOI: 10.5281/zenodo.20743173
Fatiha. I et al / vol. 01, n°1 - 2026

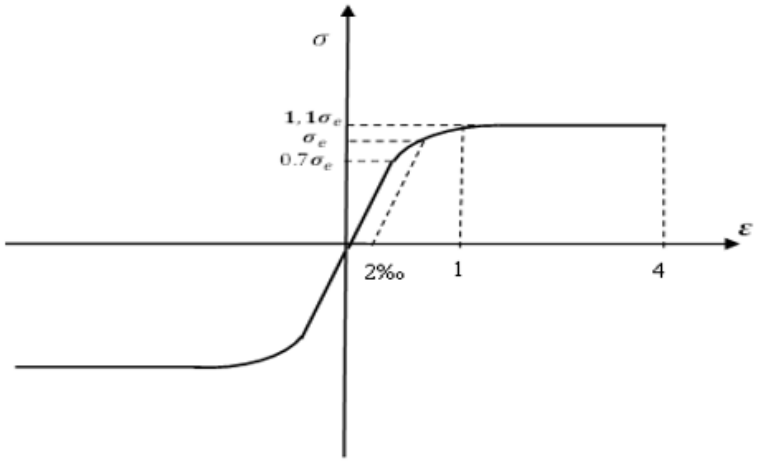

Figure 3 Behaviour of work-hardened steels

$$\sigma_s = E_a\ \varepsilon_s \text{for } \sigma_s \leq 0.7\sigma_e$$
$$\varepsilon_s = \frac{\sigma_s}{E_a} + 0.823\left(\frac{\sigma_s}{\sigma_e} - 0.7\right)^5 \text{ for } 0.7\sigma_e < \sigma_s < 1.1\sigma_e \quad (3)$$
$$\sigma_s = 1.1\sigma_e \text{for } 1\backslash\text{permil} < \varepsilon_s < \varepsilon_r$$

Where:

E_a: is the initial Young's modulus of the steel

σ_e: is the conventional 2% yield strength

$0.7\sigma_e$: is the stress at which the linear part of the diagram ends

- **Constitutive Behavior of Prestressing Steel**

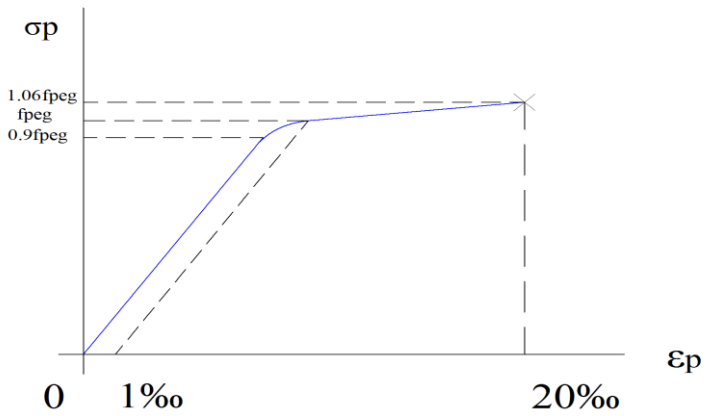

Algerian Journal of Chemical Engineering
EISSN: 2773-3068 (Online)
DOI: 10.5281/zenodo.20743173
Fatiha. I et al / vol. 01, n°1 - 2026

Figure 4 Constitutive Behavior of Prestressing Steel

$$\sigma_p = E_p.\varepsilon_p \qquad \text{pour } 0 < \sigma_p < 0.9f_{peg}$$

$$\varepsilon_p = \frac{\sigma_p}{E_p} + 100.\left(\frac{\sigma_p}{f_{peg}} - 0.9\right)^5 \qquad \text{pour } 0.9f_{peg} \le \sigma_p < 1{,}1f_{peg} \qquad (4)$$

$$\sigma_p = 1{,}01f_{peg} \qquad \text{pour } \varepsilon_p \ge 0.02$$

Where:

σ_p: stress in the prestressing steel

ε_p: strain in the prestressing steel

E_p: initial Young's modulus of steel

f_{peg}: conventional yield strength at 0.1% strain

$0.9f_{peg}$: stress at which the linear elastic branch ends

$1.06f_{peg}$: ultimate (rupture) stress

2.2 Section Equilibrium

The section is discretized into a series of segments, Each part of the structure is discretized into beam elements. The Geometric description of the cross-section is given by:

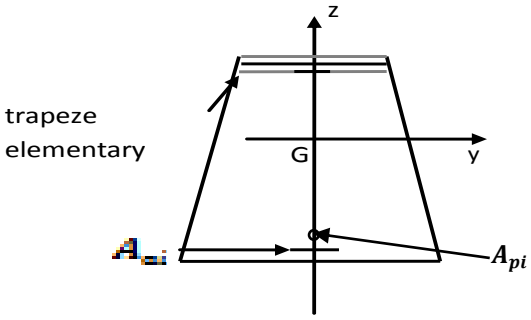

Figure 5 Discretization of the section into trapezoidal segments

The element calculation is using the given following relation:

$$\begin{pmatrix}\Delta F_{sn}\\ \Delta F_{st}\end{pmatrix} + \begin{pmatrix}A_{pn}\\ A_{pt}\end{pmatrix} = [K_s].\begin{pmatrix}\Delta\varepsilon_n\\ \Delta\varepsilon_t\end{pmatrix}, \qquad (5)$$

where $\Delta \boldsymbol{F}_{sn}$ and $\Delta \boldsymbol{F}_{st}$ are normal forces increase and shear forces increasing .

$\Delta\varepsilon_n$ $\Delta\varepsilon_t$ the normal and tangential strains increase

$\left[\boldsymbol{K}_s\right]$: cord sections stiffness matrix

Algerian Journal of Chemical Engineering
EISSN: 2773-3068 (Online)
DOI: 10.5281/zenodo.20743173
Fatiha. I et al / vol. 01, n°1 - 2026

Section equilibrium expresses that the increment of external actions and the effect of prestressing are balanced by the increment of internal forces.

$$[K_s] = \begin{bmatrix} [K_{mn}] + [K_{fn}] & [K_{fnt}] \\ {}^{t}[K_{fnt}] & [K_{mt}] + [K_{ft}] \end{bmatrix} \quad (6)$$

For each load step, the incremental nodal displacements $\{\Delta U\}$ are obtained by solving the linearized form of the nonlinear system:$\{\Delta P\} = [K]\{\Delta U\}$

In the case of prestressing, the equilibrium equation can be written as:

$\{\Delta P\} + \{A\} = [K]\{\Delta U\}$

where $\{A\}$ denotes the equivalent nodal force vector induced by the prestressing effects.

In the case of prestressing, the term [Kfn] and $[K_{ft}]$ is added in Equation (4)

where $[\boldsymbol{K}_{mn}]$ is cord stiffness matrix linked the increase of the normal forces and the sections normal strains increase.

$$[\boldsymbol{K_{mn}}] = \int \boldsymbol{E_m}(\boldsymbol{y},\boldsymbol{z}).\begin{bmatrix} \boldsymbol{1} & \boldsymbol{z} & \boldsymbol{y} \\ \boldsymbol{z} & \boldsymbol{z^2} & \boldsymbol{yz} \\ \boldsymbol{y} & \boldsymbol{yz} & \boldsymbol{y^2} \end{bmatrix}.\boldsymbol{dS_m} \quad (7)$$

$[\boldsymbol{K}_{mt}]$:cord stiffness matrix given by:

$$[\boldsymbol{K}_{mt}] = \begin{bmatrix} G \cdot A_y & 0 & 0 \\ 0 & G \cdot A_z & 0 \\ 0 & 0 & G \cdot I_x \end{bmatrix} \quad (8)$$

where G denotes the shear modulus : $G = \frac{E}{2(1+\upsilon)}$

A_y *and* A_z are the reduced shear areas associated with the shear forces

$$[K_{fn}] = \sum_{i=1}^{n_f} E_{fi}.cos^3\alpha i.s_{fi}.\begin{bmatrix} 1 & z_{fi} & y_{fi} \\ z_{fi} & z^2{}_{fi} & y_{fi}z_{fi} \\ y_{fi} & y_{fi}z_{fi} & y^2{}_{fi} \end{bmatrix} \quad (9)$$

α_i is the angle between the reinforcement of order i and the $G_x$axis.

s_{fi} is the cross sectional area of the reinforcement of order i.

E_{fi} the modulus relating the increment in stress to the increment in strain of the reinforcement of order i

$$[\boldsymbol{K}_{ftn}] = [\boldsymbol{K}_{fnt}]^t \quad (10)$$

$$[\boldsymbol{K}_{ft}] = \sum_{i=1}^{n_f} E_{fi} \cdot \sin^2\alpha i \cdot s_{fi} \cdot V_{fti} \cdot {}^tV_{fti} \quad (9)$$

Algerian Journal of Chemical Engineering
EISSN: 2773-3068 (Online)
DOI: 10.5281/zenodo.20743173
Fatiha. I et al / vol. 01, n°1 - 2026

$$V_{fti} = \begin{pmatrix} cos\beta_i \\ sinB_i \\ (y_{fi} - y_c)sin\beta i - (z_{fi} - z_c)cos\beta i \end{pmatrix} \quad (10)$$

β_i represents the angle formed by the projection of the reinforcement of order $i$in the cross-sectional plane with the y axis.

-External loads

The cross-section of a beam element is subjected to an increment of external loading, which is given by:

$$F_{sn} = \begin{pmatrix} N \\ M_y \\ M_z \end{pmatrix} \quad (11)$$

$$F_{st} = \begin{pmatrix} T_y \\ T_z \\ M_{cx} \end{pmatrix} \quad (12)$$

Moreover, the cross-section is subjected to the action of prestressing, which can be decomposed into parts.

$$A_{sn} = -\sum_{i=1}^{n_{fp}} \sigma_{pi} . \begin{pmatrix} 1 \\ z_{pi} \\ y_{pi} \end{pmatrix} . cos\alpha_i \, S_{fpi} \quad (13)$$

$$A_{st} = -\sum_{i=1}^{n_{fp}} \sigma_{pi} . \begin{pmatrix} cos\beta_i \\ sin\beta_i \\ y_{pi}sin\beta_i - z_{pi}cos\beta_i \end{pmatrix} . sin\alpha_i \, S_{fpi}$$ where n_{fp}

(14)

- The equilibrium of the section is determined by evaluating the determinant of the sectional stiffness matrix $[K_s]$and checking the reinforcement failure criteria. If these conditions are satisfied, the system of equations is solved:

$\{\Delta F_s\} + \{A_p\} = [K_s] \cdot \{\Delta \varepsilon_s\}$

(15)

Then, a convergence check is performed.

Algerian Journal of Chemical Engineering
EISSN: 2773-3068 (Online)
DOI: 10.5281/zenodo.20743173
Fatiha. I et al / vol. 01, n°1 - 2026

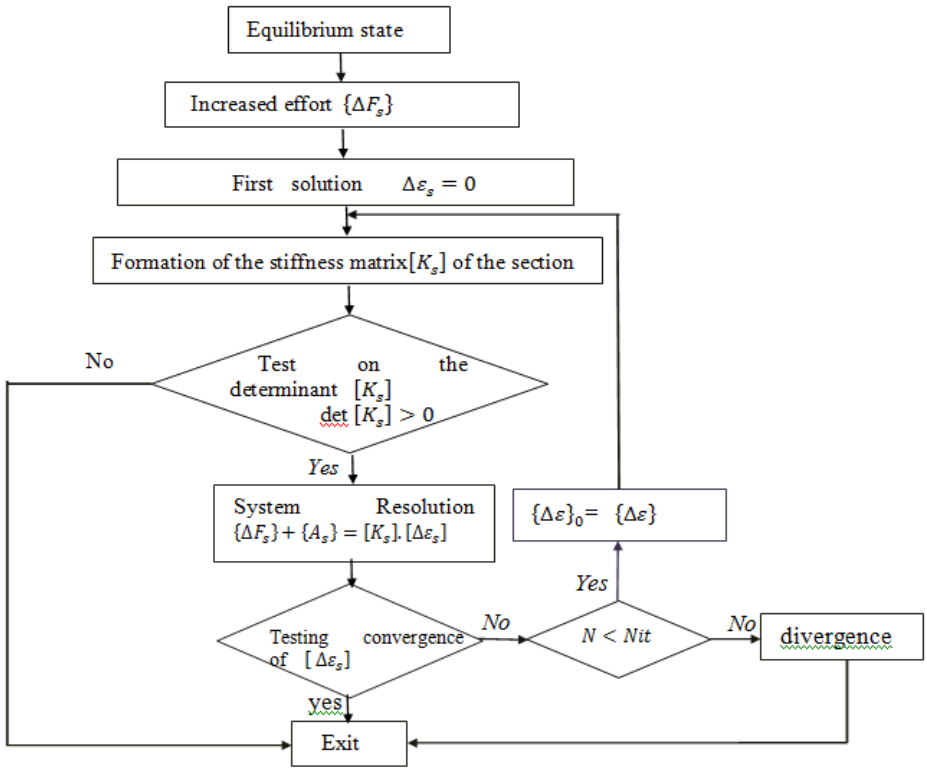

Figure 6 Flow chart of the procedure for the research of equilibrium section

3 Numerical Procedure for Nonlinear Structural Analysis

The structure's stiffness matrix [$\boldsymbol{K}$] is formed from the element's stiffness matrix [$\boldsymbol{K}_X$] in the absolute axis. The element stiffness matrix [$\boldsymbol{K}_X$] is given from the section stiffness matrix in the calculated in the intrinsic axis system. For each loading step, the problem is to calculate the nodes displacement increase $\{\Delta \boldsymbol{U}\}$ by solving of the following nonlinear system witch describe the structure equilibrium: $\Delta P = [\boldsymbol{K}]\ \{\Delta \boldsymbol{U}\}$ (16)

The nonlinear finite element analysis is conducted according to the following computational procedure:

- Finite element discretization of the beam
- Formulation of the sectional stiffness matrix
- Incorporation of prestressing effects
- Assembly of the global stiffness matrix
- Application of boundary conditions and external loads
- Incremental-iterative nonlinear solution procedure
- Convergence check at each load step
- Post-processing and evaluation of results

Algerian Journal of Chemical Engineering
EISSN: 2773-3068 (Online)
DOI: 10.5281/zenodo.20743173
Fatiha. I et al / vol. 01, n°1 - 2026

3 . Results and Discussions

3.1 Continuous beam

The continuous beam test (OH4) was conducted at CEBTP by Y. Bouafia [04]. The beam features a double T-shaped cross-section, rests on two simple supports spaced 3.75 m apart, and is extended by a 1.25 m cantilever. The laboratory experiment is described in detail in Ref. [04]. The mechanical characteristics measured on the samples are presented in tables 3.

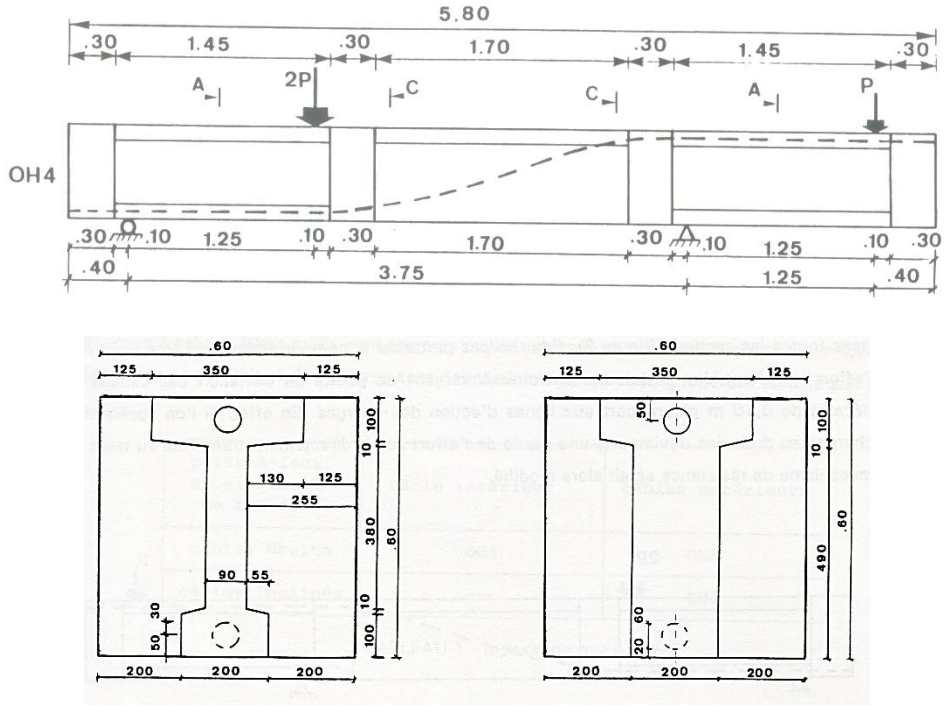

Figure 7 Construction details of the beam

Table 3. Mechanical characteristics of concrete (Bouafia [04]).

Reference	Age ($days$)	Module E_{b0}(MPa)	Stress f_{cj}(MPa)	ε_{b0}(٪)	f_{ij} (MPa)
OH4	37	32070,00	34,50	0 ,16	3,30

The passive reinforcement of beam OH4 is made of cold-worked steel with a diameter of 5 mm. Prestressing is applied by post-tensioning. The cable is composed of 6 strands of Ø13 mm and is placed inside a flexible jacket. The initial prestressing force at the anchorage is 556 kN.
Results and interpretation

Algerian Journal of Chemical Engineering
EISSN: 2773-3068 (Online)
DOI: 10.5281/zenodo.20743173
Fatiha. I et al / vol. 01, n°1 - 2026

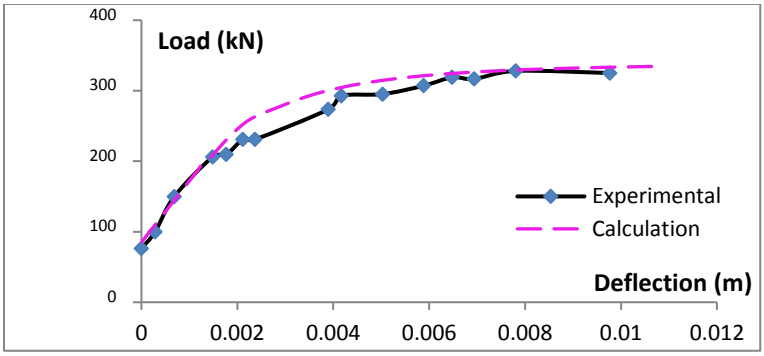

Figure 8 Load-deflection curve for the beam OH4

The numerical curve closely matches the experimental curve, indicating that the modeling accurately predicts the structural behavior.

3.2 Prestressed concrete beam

This is a testing program that was undertaken in 1976 by TRINH [14] at the Building and Public Works Research Center (CEBTP) by the Structural Studies Department (SES).

The HZ3 beam, one of the four beams in the test, is subjected to an increasing load until failure. It has an I-shaped cross-section and a total length of 10.4 m, consisting of two equal spans of 5 m each. Two concentrated loads of equal magnitude Q are applied at the midspan of each span. The figure shows the geometric characteristics of the beam

.

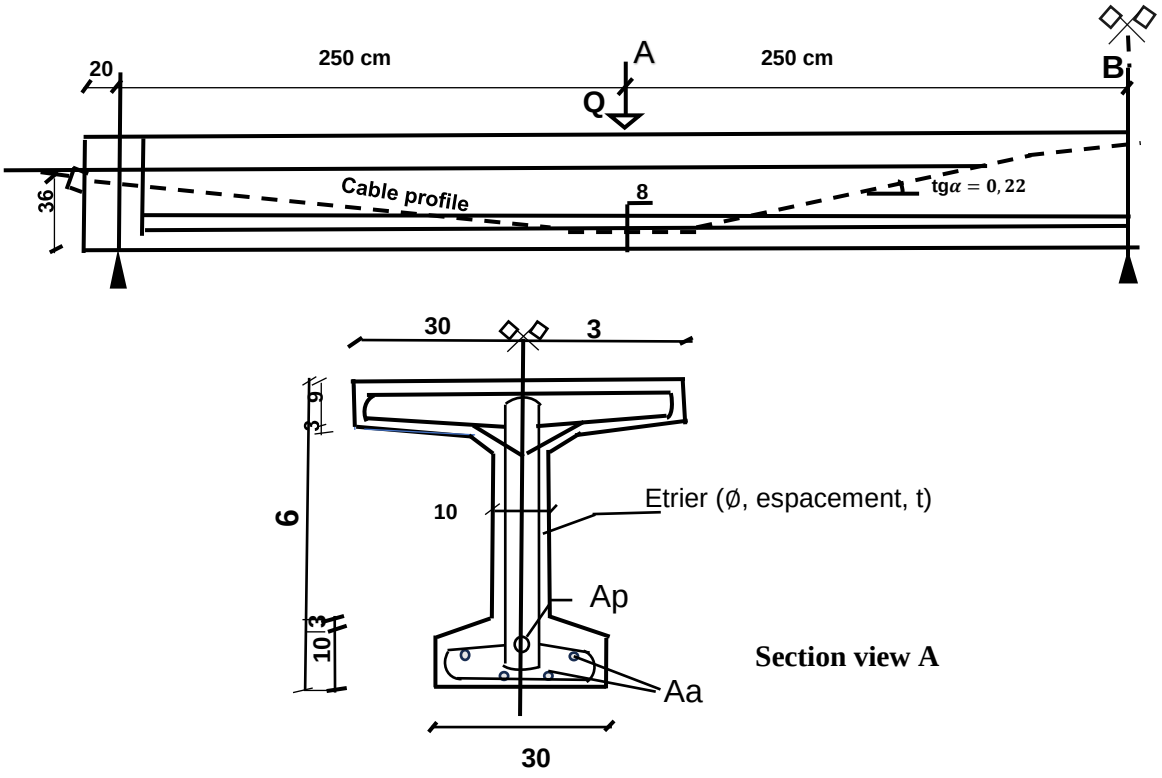

Algerian Journal of Chemical Engineering
EISSN: 2773-3068 (Online)
DOI: 10.5281/zenodo.20743173
Fatiha. I et al / vol. 01, n°1 - 2026

Figure 9. Formwork and reinforcement of HZ beams

Table 1 HZ Beam

Parameter	1	2	3
Aa	–	4T16	4T20 + 1T25 + 2T20
B	–	4T20	5T25
ha	A	–	56
hb	B	56	56
Ap	1087	1007	707
Stirrups t	18	16	15

Table 2 Characteristics of concrete and passive reinforcement of HZ 1, HZ 2 and HZ 3 beam

Beam index	$f_{tj}(MPa)$	$f_{ij}(MPa)$	$E_{ij}(MPa)$	Bars	f_e	E_a	$f_u\ (MP\ a)$
HZ1	39	3.4	35400	∅6	340	206	435
HZ2	33	3.0	31250	HA10	428	198	545
HZ3	34	3.4	32080	HA16	430	213	526

The behavior of concrete in compression is modeled using the Sargin law, taking

K= $\frac{E_{b0}\cdot\varepsilon_{b0}}{f_{cj}}$ and $K' = \frac{(\mathrm{K}-1)(55-\mathrm{f_{cj}})}{25}$

The strain corresponding to f_{cj} is taken as equal to $2.f_{cj}/E_{b0}$

The HZ beams were the subject of a numerical study [14]. The HZ1 beam, which is the most highly prestressed, is nevertheless provided with a minimum amount of passive reinforcement, consisting of continuous smooth 6 mm bars (FeE 22 steel). No longitudinal reinforcement is present in the web. Each specimen includes transverse reinforcement arranged in successive sections with a constant spacing *t*.

Prestressing is achieved by post-tensioning. The cables are composed of a variable number of 7 mm wires, corresponding respectively to the HZ1, HZ2, and HZ3 beams. A single cable is placed in each beam within a duct of 34 mm diameter. The average mechanical properties of the 7 mm wire, obtained from tensile tests on samples. The initial anchorage stress σ_0 is 1142 MPa, taking into account prestress losses due to time-dependent effects in the concrete between prestressing and testing. Friction losses along the cable are automatically computed by the program, using friction and wobble coefficients (

$f = 0.15$and $\varphi = 0.0004$ rad/m)

Algerian Journal of Chemical Engineering
EISSN: 2773-3068 (Online)
DOI: 10.5281/zenodo.20743173
Fatiha. I et al / vol. 01, n°1 - 2026

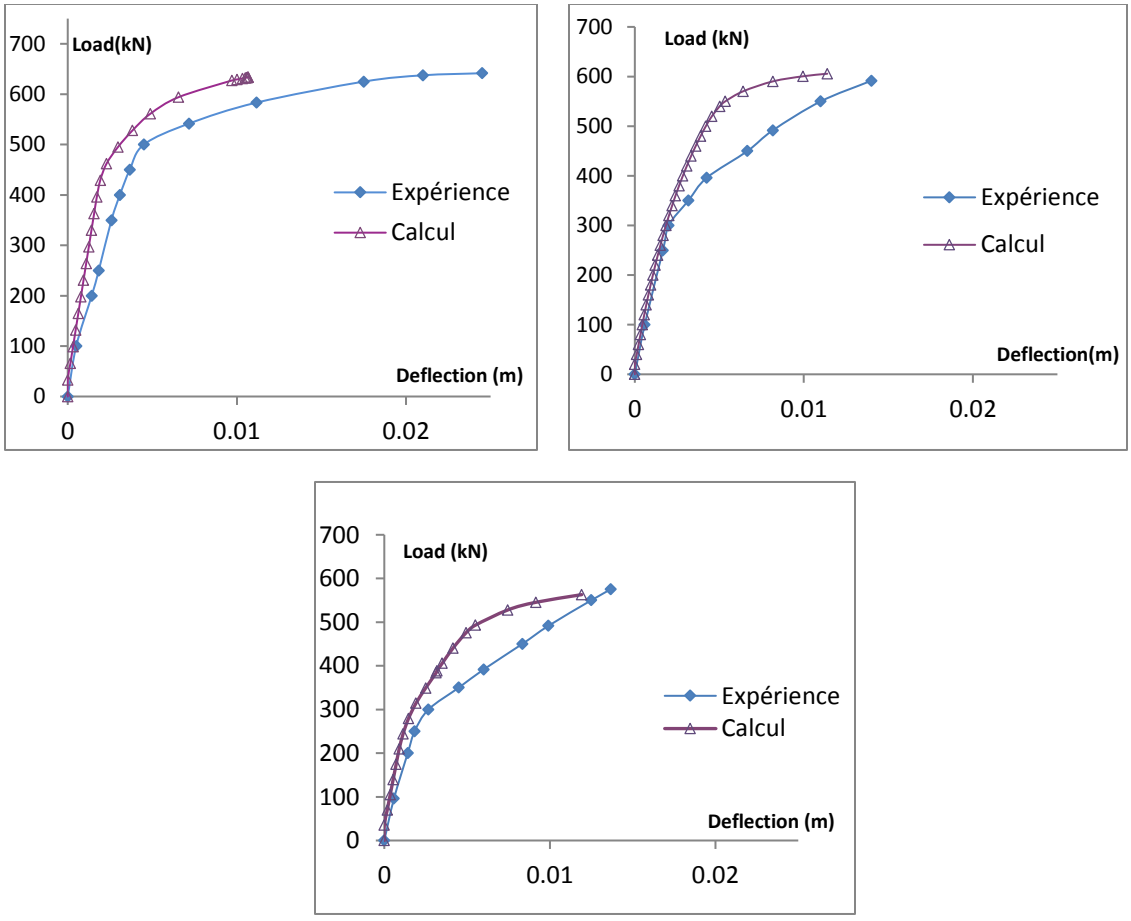

Figure 8 Load-deflection curve for the beam HZ1, HZ2 and HZ3

The HZ2 and HZ3 beams failed in shear, while the HZ1 beam failed in bending.
In the case of flexural failure (HZ1), the calculated curve closely matches the experimental curve, with a slight deviation observed in the nonlinear range.
For the beams that failed in shear, a significant discrepancy is observed between the experimental and calculated curves. This is mainly due to the fact that shear deformations are neglected in the model.

3. Conclusion

This study focused on prestressed concrete structures. In particular, it dealt with the formulation of the sectional stiffness matrix for reinforced concrete beams. This required the introduction of transformations between different coordinate systems. This section presents the failure modes of the tested beams and compares the experimental results with the numerical responses. The results show good agreement between numerical simulations and experimental data. These improvements led to satisfactory outcomes, especially regarding the effect of prestressing on structural behavior.

Algerian Journal of Chemical Engineering
EISSN: 2773-3068 (Online)
DOI: 10.5281/zenodo.20743173
Fatiha. I et al / vol. 01, n°1 - 2026

Nomenclature

$[K]$ Stiffness matrix

$\{\Delta U\}$ Vector of nodes displacements increase

$\{\Delta F\}$ Vector nodes forces increase

$\{\Delta P\}$ Vector of applied loads increase

$\{\Delta S\}$ Vector of nodes displacements increase

[**K**s] Sections Stiffness matrix

[**S**s] Sections flexibility matrix

E_a Elastic modulus of passive reinforcement

E_{b0} Elastic modulus of concrete

f_{cj} Concrete compressive strength at *j* day

f_{tj} Concrete tensile strength at *j* day

ε_{b0} Peak of the strains corresponding t_0 f_{cj}

K_b and K_b' Dimensionless parameters of the Sargin low

u, *v* Longitudinal displacements of thenodes

ε Longitudinal deformation

σ_e Elastic stress from passive steel

σ_r Tensile strength of steel reinforcement

θ_x The angle of torsion

α Angle between the center line of the reinforcement and the axis *Gx*

β Angle between the reinforcement, projection in the plane of the section and the axis *Gy*

(y_f , z_f) The reinforcement crossing point in the coordinate *Gyz* axis system

$\{\Delta\varepsilon_n\}$ Normal strains increase

$\{\Delta\varepsilon_t\}$ Shear strains increase

$E_m(y,z)$ Concrete modulus

$[S_s]$ The flexibility matrix of the section, βi The angle between the projection of the reinforcement bare *i* in the plan G_{yz}, and the axis G_y

(y_{fi}, z_{fi}) The coordinate of the reinforcement bare *i* in the axis system G_{yz}

α_i the angle between of the reinforcement bare *i* and the axis G_x

s_{fi} The cross-section of the reinforcement bare *i*

E_{fi} The elastic modulus of the reinforcement

Declarations

This research received no specific grant from any funding agency.
The authors declare that they have no conflict of interest.

References

1. Bouafia, Y. *Simulation numérique du comportement moyen jusqu'à la rupture d'une zone de poutre : application au béton armé ou précontraint et au béton fibré*. Mémoire de DEA, Université Pierre et Marie Curie (Paris VI), Juin 1987.
2. Bouafia, Y., Fouré, B., et Kachi, M.S. *Shear Strength of Externally Prestressed Beams*. Proceedings of the II International Symposium on Cement and Concrete Technology in the 2000s, Turkish Cement Manufacturers' Association and European Cement Association, Istanbul, Turkey, 6–10 Septembre 2000, Vol. 2, pp. 522–531, ISBN : 975-8136-09-7.
3. Felippa, C.A. *Nonlinear Finite Element Methods*. University of Colorado Boulder, Colorado 80309-0429, USA, Août 2001.
4. Bouafia, Y. *Résistance à l'effort tranchant des poutres en béton à précontrainte extérieure : étude expérimentale et calcul à la rupture*. Thèse de Doctorat, École Centrale des Arts et Manufactures, Paris, France, Novembre 1991.
5. Virlogeux, M., et M'Rad, A. *Étude d'une section de poutre en élasticité non linéaire : application au béton armé ou précontraint et aux sections mixtes*. Annales de l'Institut Technique du Bâtiment et des Travaux Publics.
6. Iguetoulene, F., Bouafia, Y., et Kachi, M.S. *Nonlinear Modeling of Three-Dimensional Reinforced and Fiber Concrete Structures*. Frontiers of Structural and Civil Engineering, 2017.
7. Bouafia, Y., Kachi, M.S., et Fouré, B. *Relation contrainte–déformation dans le cas du béton armé de fibres d'acier*. Annales du BTP, n° 2, Éditions ESKA, France, 1998, pp. 5–17, ISSN 1270-9840.
8. Grelat, A. *Analyse non linéaire des ossatures hyperstatiques en béton armé*. Thèse de Docteur Ingénieur, Université Paris VI, 1978.
9. Nait-Rabah. *Simulation numérique des ossatures spatiales*. Thèse de Doctorat, École Centrale de Paris, 1990.
10. Riks, E. *The Application of Newton's Method to the Problem of Elastic Stability*. Journal of Applied Mechanics, Vol. 39, 1972, pp. 1060–1066.

11. Zhan. *Contribution au dimensionnement des pieux en béton de fibres*. Thèse de Doctorat, Laboratoire CEBTP, 1991.

12. Iguetoulene, F., Bouafia, Y., et Kachi, M.S. *Incremental Analysis for the Nonlinear Buckling Responses of the Reinforced Concrete and the Steel Spatial Arch Truss Structure Subjected to Displacement Dependent Loads*. International Journal of Structural and Civil Engineering Research, Mars 2024.

13. Adjrad, A., Kachi, M.S., Bouafia, Y., et Iguetoulene, F. *Nonlinear Modeling Structures on 3D*. Proceedings of the 4th Annual ICSAAM, pp. 1–9.

14. Trinh, J.L. *Précontrainte partielle : de la théorie à la pratique*. Annales de l'Institut Technique du Bâtiment et des Travaux Publics, No. 444, Mai 1986.